

Heat-current correlation loss induced by finite-size effects in a one-dimensional nonlinear lattice

Lei Wang (王雷),* Lubo Xu (续路波), and Huizhu Zhao (赵会铸)

Department of Physics and Beijing Key Laboratory of Opto-electronic Functional Materials and Micro-nano Devices, Renmin University of China, Beijing 100872, People's Republic of China

(Received 22 August 2014; revised manuscript received 13 October 2014; published 7 January 2015)

The Green-Kubo formula provides a mathematical expression for heat conductivity in terms of integrals of the heat-current correlation function, which should be calculated in the thermodynamic limit. In finite systems this function generally decreases, i.e., it decays faster than it does in infinite systems. We compared the values of the correlation function in a one-dimensional purely quartic lattice with various lengths, and found that this loss is much smaller than is conventionally estimated. By studying the heat diffusion process in this lattice, we found that, in contrast to the conventional belief, the collisions between sound modes do not noticeably affect the current correlation function. Therefore, its loss being surprisingly small can be well understood. This finding allows one to calculate the heat conductivity in a very large system with desirable accuracy by performing simulations in a system with much smaller size, and thus greatly broadens the application of the Green-Kubo method.

DOI: [10.1103/PhysRevE.91.012110](https://doi.org/10.1103/PhysRevE.91.012110)

PACS number(s): 05.60.-k, 44.10.+i

I. INTRODUCTION

Anomalous heat conduction in low-dimensional systems has attracted rapidly increasing interest recently [1,2]. It has been generally accepted for many years, with only very few exceptions such as the coupled rotator lattice [3,4], that heat conduction in one-dimensional (1D) momentum-conserving nonlinear lattices is anomalous [1,2,5]. The heat conductivity κ in those lattices is length dependent and diverges with lattice length L as L^α with a positive α in the thermodynamic limit. The universality and detailed value of this power exponent α are still open questions, however [6–11]. Two different methods, the nonequilibrium heat-bath method and the equilibrium Green-Kubo method, are commonly applied to calculate the heat conductivity. The latter method provides a mathematical expression for heat conductivity in terms of integrals of the heat-current correlation function in equilibrium states [12]. It is theoretically simple since only the lattices themselves need to be studied. As a comparison, in the nonequilibrium heat-bath method, the heat baths must be considered as a part of the whole system, which generally makes enormous difficulties.

Practically, however, the correlation function needs to be calculated in the thermodynamic limit but any numerical simulation can be performed only in finite systems. The current correlation function in finite systems generally decays faster than in infinite ones. This loss is conventionally attributed to collisions between sound modes which occur only in finite systems. As a consequence, one is able to correctly calculate the correlation function in only a short time-lag range before sound modes collide with each other. Such a requirement seriously limits the usage of the Green-Kubo method.

II. MODEL AND SIMULATION**A. Lattice model**

In this paper we numerically study the heat-current correlation function in a one-dimensional nonlinear lattice. The

main objective is to study the finite-size effects quantitatively and reveal their true physical origin. The Hamiltonian of the system reads

$$H = \sum_i \left[\frac{\dot{x}_i^2}{2} + V(x_i - x_{i+1}) \right]. \quad (1)$$

The mass of all the particles has been set to unity. We focus on a purely quartic potential, i.e., $V(x) = \frac{1}{4}x^4$, due to its simplicity and high nonlinearity, which enable its asymptotic behaviors to be displayed in relatively short time and space scales. The interaction between particles i and $i+1$ is $f_i = -\partial V(x_i - x_{i+1})/\partial x_i$. The instantaneous local heat current $j_i \equiv \dot{x}_i(f_{i-1} + f_i)/2$, and the instantaneous global heat current $J(t) \equiv \sum_i j_i(t)$. A periodic boundary condition, which provides the best convergence to properties in the thermodynamic limit, is applied in all the simulations. Microcanonical simulations are performed with zero total momentum and identical energy density ϵ which corresponds to temperature $T = 1$. ϵ equals 0.75 for this purely quartic lattice. An embedded Runge-Kutta-Nystrom algorithm of orders 8(6) [13] is applied for this deterministic Hamiltonian system. This high-order algorithm enables us to calculate very long-time correlations with considerable good accuracy and acceptable computational resource cost.

B. Heat-current correlation loss

In a lattice with N particles, the rescaled heat-current correlation function is defined as

$$c_N(\tau) \equiv \frac{1}{k_B T^2 N} \langle J(t)J(t+\tau) \rangle_t. \quad (2)$$

The Boltzmann constant k_B is set to unity throughout this paper. Compared with $c_N(\tau)$ for finite N , its thermodynamic limit is much more important, i.e.,

$$c(\tau) \equiv \lim_{N \rightarrow \infty} c_N(\tau). \quad (3)$$

*phywanglei@ruc.edu.cn

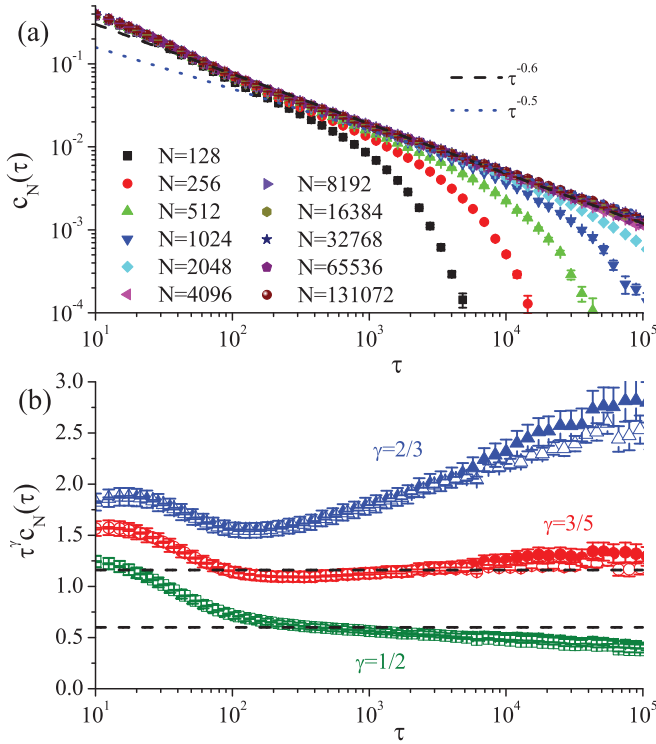


FIG. 1. (Color online) (a) Rescaled heat current correlation $c_N(\tau)$ for the purely quartic lattice versus time lag τ for various lattice length N . Data binning over contiguous τ regimes has been performed in order to reduce statistical fluctuations. Dashed and dotted lines with slope $-3/5$ and $-1/2$, respectively, are drawn for comparison. (b) $\tau^\gamma c_N(\tau)$ for various values of γ . Three groups of symbols from the top down along the vertical axis correspond to $\gamma = 2/3$, $3/5$, and $1/2$, respectively. Solid symbols correspond to $N = 131072$ and the open ones correspond to $N = 65536$. In order to avoid confusion only the data for those two longest N are plotted. Two horizontal dashed lines are drawn for reference. It is clearly seen that the curve in middle ($\gamma = 3/5$) is the most horizontal one in the wide range of $\tau \in (10^2, 10^5)$.

According to the Green-Kubo formula, the heat conductivity can be determined as

$$\kappa_{GK} \equiv \int_0^\infty c(\tau) d\tau. \quad (4)$$

In the anomalous heat conduction case where the above integral does not converge, the length-dependent heat conductivity is calculated by setting a cutoff time as the upper limit of the integral, i.e.,

$$\kappa_{GK}(L) \equiv \int_0^{L/v_s} c(\tau) d\tau. \quad (5)$$

v_s is the speed of sound, which equals about 1.23 in this purely quartic model [14].

In practice, only lattices with finite N can possibly be simulated, and the rescaled heat-current correlation function $c_N(\tau)$ generally varies with the lattice length N . Therefore, the finite-size effect must be taken into careful consideration. It is well known and can be observed in Fig. 1(a) that this finite-size effect has the following effects: (1) $c_N(\tau) < c(\tau)$; (2) the shorter the N , the faster $c_N(\tau)$ decays; and (3) the longer

τ , the larger the effect. The conventional belief (hereinafter referred to as “the belief”) is that $c_N(\tau)$ is acceptably close to $c(\tau)$ only when $\tau < \tau_{col}(N) \equiv \frac{N}{2v_s}$; see for example Ref. [15]. According to the belief and Eq. (5), in order to determine $\kappa_{GK}(L)$ one needs to simulate a lattice with twice the length of L . This condition seriously limits the application of the Green-Kubo method. That is why the Green-Kubo formula is commonly deemed to be an inefficient way of determining the heat conductivity, and thus has been rarely applied in numerical simulations. We shall reveal that this belief is questionable in this lattice.

To this end, we define $\Delta c_N(\tau)$, the heat-current correlation loss (CCL) induced by the finite-size effect, as

$$\Delta c_N(\tau) \equiv c(\tau) - c_N(\tau). \quad (6)$$

The relative CCL is defined as

$$\lambda_N(\tau) \equiv \frac{\Delta c_N(\tau)}{c(\tau)} = 1 - \frac{c_N(\tau)}{c(\tau)}. \quad (7)$$

We also define a characteristic time lag, the cutoff time lag $\tau_c(N)$, as the value at which the relative loss $\lambda_N(\tau)$ approaches a certain critical value η , namely,

$$\lambda_N(\tau_c(N)) = \eta. \quad (8)$$

We first need to determine the value of $c(\tau)$ with a desired accuracy in a certain range of τ before we are able to calculate all the quantities $\Delta c_N(\tau)$, $\lambda_N(\tau)$, and $\tau_c(N)$. We temporarily accept the belief, based on which a lattice with $N = 131072$ is long enough to correctly determine $c(\tau)$ when $\tau \leq \frac{131072}{2v_s} \approx 5 \times 10^4$. We will see that such a requirement is too conservative and is not necessary indeed for the lattice that we studied. For simplicity, $c(\tau)$ refers to $c_{131072}(\tau)$ in the descriptions of our numerical simulations hereafter.

The relative CCL $\lambda_N(\tau)$ for various lattice lengths N is plotted in Fig. 2(a). We see that $\lambda_N(\tau)$ increases faster in shorter lattices. Quite intriguingly, all the data of $\lambda_N(\tau)$ for various N fit the following universal relation very well:

$$\lambda_N(\tau) \approx 3N^{-1.16} \tau^{0.58}. \quad (9)$$

This relation indicates that the cutoff time lag $\tau_c(N)$ follows a square-law dependence on the lattice length N :

$$\tau_c(N) \approx \left(\frac{\eta}{3}\right)^{1/0.58} N^2. \quad (10)$$

If we set $\eta = 0.1$, namely, $c_N(\tau)$ decreases to 90% of $c(\tau)$ when $\tau = \tau_c(N)$, then

$$\tau_c(N) \approx 2.84 \times 10^{-3} N^2. \quad (11)$$

In Fig. 2(b) we see that such an expectation agrees with the numerical data very well.

Since $\tau_c(N)$ satisfies the square law so well in the range of N that we have studied, it is reasonable to expect that this relation remains valid in an even larger N range. In our previous work [14], the longest lattice that we simulated was $N = 2 \times 10^4$. Since $\tau_c(2 \times 10^4) = 1.14 \times 10^6$ is longer than the longest τ ($= 1 \times 10^6$) that we studied in that reference, the relative CCL induced by the finite size effect is therefore no more than 10%. How much the calculation of the decay power exponent $\gamma \equiv \frac{d \ln c(\tau)}{d \ln \tau}$ is affected by the 10% CCL depends

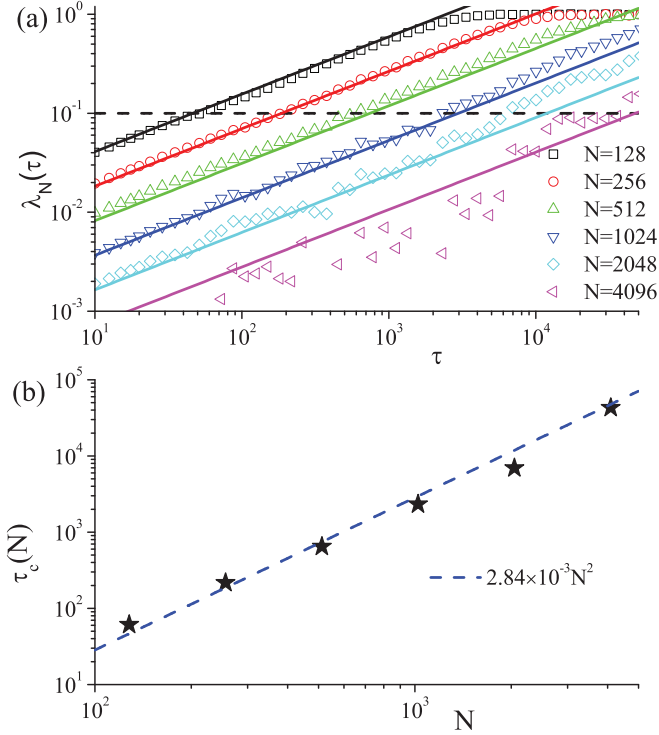


FIG. 2. (Color online) (a) $\lambda_N(\tau)$ as a function of τ for various lattice length N . Oblique solid lines from the top down stand for the fittings of $\lambda_N(\tau)$, $3N^{-1.16}\tau^{0.58}$, for N ranging from 128 to 4096. The horizontal dashed line refers to $\lambda_N(\tau) = 0.1$. The functions of $\lambda_N(\tau)$ cross this line at the cut-off time lag $\tau_c(N)$. (b) The cut-off time lag $\tau_c(N)$ as a function of the lattice length N . The blue dashed line stands for $2.84 \times 10^{-3} N^2$.

on the regime of τ in which the data is fitted. Given the fact that γ was fitted over four orders of magnitude of τ [see Fig. 2(a) in Ref. [14]], the underestimate of γ induced therefrom must be lower than $|\log_{10} 0.9|/4 \approx 0.01$. Because such an error is much smaller than the difference between $-2/3$ and $-3/5$, it would not affect the main conclusion in the Ref. [14]. We expect that the cases in two-dimensional [16] and three-dimensional [17] purely quartic lattices are also similar.

In order to observe the asymptotic decay exponent of $c(\tau)$, we have plotted $t^\gamma c_N(\tau)$ in Fig. 1(b) for $\gamma = 2/3, 3/5$, and $1/2$, respectively. The relative CCL for $N = 13\,1072$ and $\tau = 10^5$ is no more than 0.28%, which is negligible. Clearly the curve in the middle, which corresponds to $\gamma = 3/5$, is the flattest one. This reconfirms our conclusion in Ref. [14] that the asymptotic decay of $c(\tau)$ follows $\tau^{-3/5}$ [1] better than $\tau^{-2/3}$ [6] and $\tau^{-1/2}$ [8,11,18]. The numerical calculation was mainly performed on one or more Nvidia Tesla-2075 graphics processing units (GPUs), each of which has 448 Cuda processing cores on board. The part of the calculation for $N = 13\,1072$ alone costs more than half a year of wall-clock time on four GPUs. The huge cost enables us to reduce the statistical uncertainty to a much lower level, compared with that in other existing studies. Since this purely quartic lattice can be regarded as the high-nonlinearity limit of the Fermi-Pasta-Ulam (FPU)- β lattice, we expect that the decay of $c(\tau)$ in the latter lattice should asymptotically tend to the same exponent, although probably on much longer time scales.

Now we go back to reconsider the above-mentioned conventional belief that $c_N(\tau)$ is sufficiently close to $c(\tau)$ only when $\tau < \tau_{col}(N) \equiv \frac{N}{2v_s}$. The physical origin of this belief can be understood by studying the energy diffusion process in an initially thermalized lattice that undergoes a δ -function-type heat pulse [19,20]. The local energy-density spreading profile in such a 1D nonlinear momentum-conserving lattice consists of a central peak (heat mode) and two side peaks (sound modes) that move with the constant speed of sound v_s . The quite different behaviors of the two kinds of modes have been recently studied by nonlinear hydrodynamic fluctuation analysis [21]. In a lattice with length N and periodic boundaries, the two sound modes approach the boundaries and collide with each other at the time $\tau_{col}(N) = \frac{N}{2v_s}$. At first glance, such a collision, which does not exist in a lattice with infinite length, affects the diffusion process badly and thus should be responsible for the CCL that is observed in Fig. 2(a).

However, if such a picture is correct, then one would expect that (1) the CCL at $\tau < \tau_{col}(N)$ should not be noticeable; (2) the change of the CCL at the time point $\tau_{col}(N)$ should be discontinuous; and (3) the cutoff time lag $\tau_c(N)$ should be proportional to the lattice length N . However, we see in Figs. 2(a) and 2(b) that (1) CCL can be distinctly observed even when $\tau < \tau_{col}(N)$; and (2) everything goes on smoothly at the time point $\tau_{col}(N)$, i.e., no discontinuity in the curves $c_N(\tau)$, $\Delta c_N(\tau)$, and $\lambda_N(\tau)$ can be observed— $\lambda_N(\tau)$ depends on τ in the same way before and after the time point $\tau_{col}(N)$; and (3) $\tau_c(N)$ is proportional not to N but to N^2 . Those observations violate the expectations completely, thus indicating that the role of the collision is not so important as was commonly expected.

C. Collision between sound modes

Now we quantitatively study the role of the collision. We have simulated the energy diffusion process for $t = 100, 150, 200$, and 300 in a lattice with length $N = 451$ and periodic boundary conditions [22]. The energy distribution profiles $p_{451}(i, t)$ at different time points are plotted in Fig. 3 (the solid symbols). The sound modes approach the boundaries $i = \pm 225$ at $t = \tau_{col}(451) = \frac{451}{2 \times 1.23} \approx 180$. Around this time point the sound modes meet, collide with each other, move out of one end of the lattice, and then move in through the other end of the lattice. In order to study the effect of the collision, we hope to build a virtual lattice with the same length $N = 451$, in which the sound modes do not interact with each other, however.

To this end, we have simulated a longer lattice with length $N = 901$. The dashed lines in Fig. 3 stand for its energy profile $p_{901}(i, t)$. In the whole time range $t \leq 300$, the sound modes do not arrive at the lattice boundaries $i = \pm 450$ and thus $p_{901}(i, t)$ tells us how the energy is distributed if the sound modes do not meet and collide. The dashed lines overlap the solid symbols very well when $t < \tau_{col}(451)$ because in both the long and short lattices the sounds have not met. The next step is easy; we simply imagine that in the long lattice the energy that moves out through $i = 225$ moves back through $i = -225$, and vice versa. Namely, $p'_{451}(-225, t) \equiv p_{901}(-225, t) + p_{901}(226, t)$, $p'_{451}(-224, t) \equiv p_{901}(-224, t) + p_{901}(227, t)$, and so on. Based on this we are able to predict the energy profile in the virtual lattice with a short length $N = 451$, $p'_{451}(i, t)$ from the

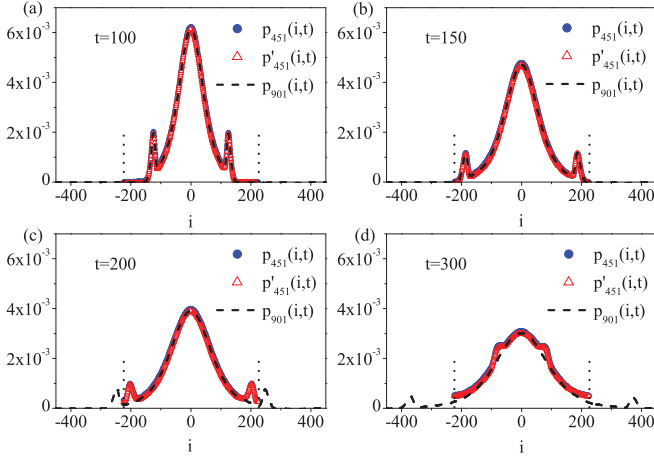


FIG. 3. (Color online) The energy diffusion profile in the real lattice $p_{451}(i, t)$ (solid blue symbols) and in the virtual lattice $p'_{451}(i, t)$ (open red symbols). $p(t)$ and $p'(t)$ always overlap with each other very well, both before and after the time of collision $\tau_{col}(451) \approx 180$. It is hard to distinguish them by eye. The two vertical dotted lines indicate the boundaries of the lattice with $N = 451$.

energy profile in the real lattice with a longer length $N = 901$, $p_{901}(i, t)$.

The comparison of the energy diffusion profiles in the real lattice $p_{451}(i, t)$ and in the virtual one $p'_{451}(i, t)$ at various time points is plotted in Figs. 3(a) to 3(d). The collision between the sound modes happens at about $t \approx 180$, i.e., the time points 100 and 150 are before the collision while the other two time points are after the collision. In all cases the discrepancy between $p_{451}(i, t)$ and $p'_{451}(i, t)$ is so small that we are not able to distinguish it from statistical fluctuation by eye. The effect of the collision between the sound modes is negligible indeed. After such a collision, no phase shift can even be observed. Compared with solitons, which undergo phase shifts after collisions, the sound modes in this 1D lattice act more like phonons rather than solitons [24].

In order to measure the small difference between $p_{451}(i, t)$ and $p'_{451}(i, t)$ quantitatively, we have calculated their root mean square deviation (RMSD),

$$\sigma(t) \equiv \sqrt{\frac{1}{N} \sum_i [p(i, t) - p'(i, t)]^2}. \quad (12)$$

It is observed in Fig. 4 that $\sigma(t)$ always stays very small, and even more importantly (1) at the time of collision, $t \approx 180$, which is indicated by the vertical dashed line, nothing unusual happens; and (2) $\sigma(t)$ for $t > 180$ is not evidently greater than that for $t < 180$. Those observations indicate strongly that the collisions between the sound modes affect the diffusion profile only very slightly. As a consequence, the heat-current correlation function is not affected noticeably, just as we have observed in Fig. 2. The relatively large values of $\sigma(t)$ at the early time can be understood by the fact that at those times p and p' are both concentrated on the central particles, and therefore the very small relative deviation between them can contribute largely to $\sigma(t)$.

Since the CCL is not mainly induced by the collision of the sound modes, it should be largely attributed to the interaction

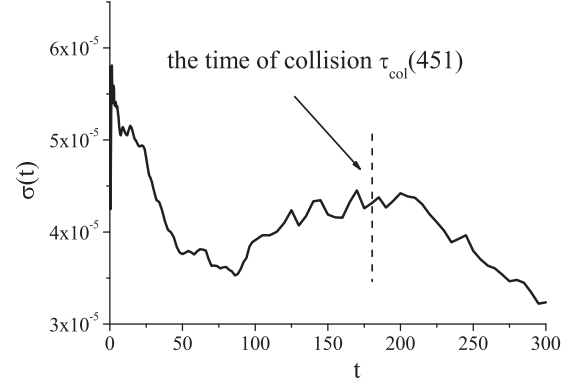


FIG. 4. The root mean square deviation $\sigma(t)$ between $p_{451}(t)$ and $p'_{451}(t)$. We do not observe anything unusual happens at the time point $\tau_{col}(451)$.

between the tails of the central peak. It has been presented that the decay of this peak satisfies the following rescaling law very well: $p(x, \mu t) \approx \mu^{-\gamma} p(\mu^{-\gamma} x, t)$ [25,26], where $\gamma \approx 0.6$. Interestingly the relative heat-current correlation loss $\lambda_N(\tau)$ depends on the time lag τ with a quite similar power exponent 0.58; see Eq. (9). More studies are necessary to understand their physical relation.

III. DISCUSSION

In summary, we have studied the heat-current correlation function and energy diffusion process in a 1D purely quartic lattice, and found that the collisions between the sound modes affect the energy distribution only negligibly. Consequently, their contribution to the heat-current correlation loss $\Delta c_N(\tau)$ is hardly noticeable. This finding allows us to calculate the correlation functions in a very long time-lag τ range with desirable accuracy by simulating a relatively much smaller system, and thus greatly broadens the application of the Green-Kubo method.

Based on this finding, we have confirmed, with a quite high accuracy, that the heat-current correlation function $c(\tau)$ in this 1D purely quartic lattice decays asymptotically as $\tau^{-0.6}$. This agrees with some theoretical analyses [1,2] and also our previous numerical simulation [14]. Since this model is the high-nonlinearity limit of a series of 1D lattice models, it is expected that the asymptotic decay power exponent is also the same in those models.

The situation is probably different in the FPU- $\alpha\beta$ lattice, because the side peaks in that model are much bigger than those in the purely quartic lattice, and they decay much more slowly. The contribution of their collisions to the CCL might be much more considerable. Furthermore, one needs to extend the measure of correlation $c(\tau)$ to a very large time lag τ in order to see the asymptotic decay of $c(\tau)$ [14,27–30].

ACKNOWLEDGMENTS

This work is supported in part by the National Natural Science Foundation of China under Grant No. 11275267. Computational resources were provided by the Physical Laboratory of High Performance Computing at Renmin University of China.

- [1] S. Lepri, R. Livi, and A. Politi, *Phys. Rep.* **377**, 1 (2003).
- [2] A. Dhar, *Adv. Phys.* **57**, 457 (2008).
- [3] C. Giardiná, R. Livi, A. Politi, and M. Vassalli, *Phys. Rev. Lett.* **84**, 2144 (2000).
- [4] O. V. Gendelman and A. V. Savin, *Phys. Rev. Lett.* **84**, 2381 (2000).
- [5] T. Prosen and D. K. Campbell, *Phys. Rev. Lett.* **84**, 2857 (2000).
- [6] O. Narayan and S. Ramaswamy, *Phys. Rev. Lett.* **89**, 200601 (2002).
- [7] T. Mai and O. Narayan, *Phys. Rev. E* **73**, 061202 (2006).
- [8] L. Delfini, S. Lepri, R. Livi, and A. Politi, *Phys. Rev. E* **73**, 060201 (2006).
- [9] S. Lepri, R. Livi, and A. Politi, *Europhys. Lett.* **43**, 271 (1998).
- [10] S. Lepri, R. Livi, and A. Politi, *Phys. Rev. E* **68**, 067102 (2003).
- [11] G. Basile, C. Bernardin, and S. Olla, *Phys. Rev. Lett.* **96**, 204303 (2006); H. van Beijeren, *ibid.* **108**, 180601 (2012).
- [12] R. Kubo, M. Toda, and N. Hashitsume, *Statistical Physics II*, Springer Series in Solid State Sciences Vol. 31 (Springer, Berlin, 1991).
- [13] J. R. Dormand, M. E. A. El-Mikkawy, and P. J. Prince, *IMA J. Numer. Anal.* **7**, 423 (1987); **11**, 297 (1991).
- [14] L. Wang and T. Wang, *Europhys. Lett.* **93**, 54002 (2011).
- [15] S. Chen, Y. Zhang, J. Wang, and H. Zhao, *Phys. Rev. E* **89**, 022111 (2014).
- [16] L. Wang, B. Hu, and B. Li, *Phys. Rev. E* **86**, 040101 (2012).
- [17] L. Wang, D. He, and B. Hu, *Phys. Rev. Lett.* **105**, 160601 (2010).
- [18] L. Delfini, S. Lepri, R. Livi, and A. Politi, *J. Stat. Mech.: Theory Exp.* (2007) P02007.
- [19] B. Li, J. Wang, L. Wang, and G. Zhang, *Chaos* **15**, 015121 (2005).
- [20] S. Chen, Y. Zhang, J. Wang, and H. Zhao, *Phys. Rev. E* **87**, 032153 (2013).
- [21] C. B. Mendl and H. Spohn, *Phys. Rev. Lett.* **111**, 230601 (2013); H. Spohn, *J. Stat. Phys.* **154**, 1191 (2014); S. G. Das, A. Dhar, K. Saito, C. B. Mendl, and H. Spohn, *Phys. Rev. E* **90**, 012124 (2014); C. B. Mendl and H. Spohn, *ibid.* **90**, 012147 (2014).
- [22] It has been proposed in Ref. [23] that the energy spatiotemporal correlation function characterizes the diffusion processes much more efficiently than does the direct diffusion simulation [19]. Therefore, what we have actually calculated are the energy spatiotemporal correlations. Please refer to Refs. [23,20] for detail.
- [23] H. Zhao, *Phys. Rev. Lett.* **96**, 140602 (2006).
- [24] N. Li, B. Li, and S. Flach, *Phys. Rev. Lett.* **105**, 054102 (2010).
- [25] P. Cipriani, S. Denisov, and A. Politi, *Phys. Rev. Lett.* **94**, 244301 (2005).
- [26] V. Zaburdaev, S. Denisov, and P. Hänggi, *Phys. Rev. Lett.* **106**, 180601 (2011).
- [27] S. Chen, Y. Zhang, J. Wang, and H. Zhao, arXiv:1204.5933.
- [28] L. Wang, B. Hu, and B. Li, *Phys. Rev. E* **88**, 052112 (2013).
- [29] S. G. Das, A. Dhar, and O. Narayan, *J. Stat. Phys.* **154**, 204 (2014).
- [30] A. V. Savin and Y. A. Kosevich, *Phys. Rev. E* **89**, 032102 (2014).